A Comparative Time Differential Perturbed Angular Correlation Study of the Nuclear Quadrupole Interaction in $HfF_4 \cdot HF \cdot 2H_2O$ Using ^{180m}Hf and ^{181}Hf(β^-)^{181}Ta as Nuclear Probes: Is Ta an Innocent Spy?

Tilman Butz[a], Satyendra K. Das[a,b], and Yurij Manzhur[a]

[a] Universität Leipzig, Fakultät für Physik und Geowissenschaften,
Institut für Experimentelle Physik II, Linnéstraße 5, D-04103 Leipzig, Germany
[b] Permanent address: Radiochemistry Laboratory, Variable Energy Cyclotron Centre,
Bhabha Atomic Research Centre, Kolkata 700064, India

Reprint requests to T. B.; E-mail: butz@physik.uni-leipzig.de

Z. Naturforsch. **64a,** 103 – 111 (2009); received May 13, 2008

We report on a comparative study of the nuclear quadrupole interaction of the nuclear probes ^{180m}Hf and ^{181}Hf(β^-)^{181}Ta in $HfF_4 \cdot HF \cdot 2H_2O$ using time differential perturbed angular correlations (TDPAC) at 300 K. For the first probe, assuming a Lorentzian frequency distribution, we obtained $\omega_Q = 103(4)$ Mrad/s, an asymmetry parameter $\eta = 0.68(3)$, a linewidth $\delta = 7.3(3.9)\%$, and full anisotropy within experimental accuracy. For the second probe, assuming a Lorentzian frequency distribution, we obtained three fractions: (1) with 56.5(7)%, $\omega_Q = 126.64(4)$ Mrad/s and $\eta = 0.9241(4)$ with a rather small distribution $\delta = 0.40(8)\%$ which is attributed to $HfF_4 \cdot HF \cdot 2H_2O$; (2) with 4.6(4)%, $\omega_Q = 161.7(3)$ Mrad/s and $\eta = 0.761(4)$ assuming no line broadening which is tentatively attributed to a small admixture of $Hf_2OF_6 \cdot H_2O$; (3) the remainder of 39.0(7)% accounts for a rapid loss of anisotropy and is modelled by a perturbation function with a sharp frequency multiplied by an exponential factor $\exp(-\lambda t)$ with $\lambda = 0.55(2)$ ns^{-1}. Whereas the small admixture of $Hf_2OF_6 \cdot H_2O$ escapes detection by the ^{180m}Hf probe, there is no rapid loss of roughly half the anisotropy as is the case with ^{181}Hf(β^-)^{181}Ta. This loss could in principle be due to fluctuating electric field gradients originating from movements of nearest neighbour HF adducts and/or H_2O molecules after nuclear transmutation to the foreign atom Ta which are absent for the isomeric probe. Alternatively, paramagnetic Ta ions could lead to fluctuating magnetic dipole fields which, when combined with fluctuating electric field gradients, could also lead to a rapid loss of anisotropy. In any case, Ta is not an "innocent spy" in this compound.

Although ^{180m}Hf is not a convenient probe for conventional spectrometers, the use of fast digitizers and software coincidences would allow to use all γ-quanta in the stretched cascade which would greatly improve the efficiency of the spectrometer. ^{180m}Hf could also serve as a Pu analogue in toxicity studies.

Key words: TDPAC; Nuclear Quadrupole Interaction; ^{180m}Hf vs. ^{181}Hf(β^-)^{181}Ta.
PACS numbers: 76.80.+y, 61.66.Fn, 61.72.-y

1. Introduction

Isomeric nuclear probes for time differential perturbed angular correlations (TDPAC) have the advantage that no nuclear transmutation occurs, i. e., no electronic re-arrangement occurs in the atomic shell. On the contrary, in electron capture (EC) decays, this re-arrangement which is accompanied by the emission of Auger electrons frequently leads to so-called after-effects, which are manifest, e. g., as a partial loss of anisotropy of the γ-γ-cascade in question. For β^--decays after-effects are not expected. In the following, we will focus on nuclear quadrupole interactions. There are three possible scenarios: (i) Neither the mother nor the daughter isotope is a constituent of the compound under investigation; in that case there could be doping problems as well as impurity-associated effects. (ii) In case the daughter isotope is a constituent of the compound under investigation, there could be doping problems only. (iii) When the mother isotope is a constituent of the compound under investigation, there are no doping problems but the daughter isotope will be a foreign atom.

It is advantageous to have a comparison between two different mother nuclei, one being an isomeric state and the other one a neighbouring isotope, which both feed cascades in one and the same daughter nucleus. A particular example is ^{111m}Cd and ^{111}In(EC)^{111}Cd. Drastic differences show up, e. g., when ^{111m}Cd and ^{111}In are substituted for a divalent metal like Cu in enzymes like the small blue copper proteins. Since In is trivalent it might not even substitute for divalent Cu or the coordination geometry is altered and after-effects show up.

^{181}Hf(β^-)^{181}Ta was widely used to study the nuclear quadrupole interaction (NQI) in a variety of compounds [1], particularly in Hf compounds. Since we have a β^--decay and since the start level of the 133 – 482 keV cascade has a half life of 17.8 μs, generally no problems associated with the nuclear transmutation are expected. Nevertheless, it often happens that a part of the anisotropy is lost within a few nanoseconds, frequently faster than the experimental time resolution. Unless a careful determination of solid angle correction factors is carried out using a liquid sample, e. g. Hf dissolved in HF, this loss is difficult to ascertain because it might be masked by minute inaccuracies in time-zero determinations and data reduction. Thus it is highly desirable to have an isomeric Hf probe for comparison.

^{180m}Hf is a candidate, however, a spectroscopically demanding one. The half life of ^{180m}Hf is 5.5 h [2], reasonably long, especially when compared to the half lives of other common isomeric probes like ^{111m}Cd ($t_{1/2} = 84.6$ min), ^{199m}Hg ($t_{1/2} = 43$ min), and ^{204m}Pb ($t_{1/2} = 66.9$ min). However, the first excited $I^\pi = 2^+$ state has a half life of only 1.5 ns which means that delayed coincidences for about 10 ns are observable only. An advantage is that the quadrupole moment is accurately known. Thus, for a proof of feasibility, we have chosen $HfF_4 \cdot HF \cdot 2H_2O$, a compound which is easy to prepare and a system which exhibits very high electric field gradients and an asymmetry parameter close to 1 where the 10 possible frequencies in the perturbation function for $I = 2$ form two groups of closely spaced lines [3]. Since the frequency resolution using this probe is not good, this greatly helps in data analysis. A further motivation for this choice is the fact that in previous studies of $HfF_4 \cdot HF \cdot 2H_2O$ using ^{181}Hf(β^-)^{181}Ta as the probe, roughly half the anisotropy is lost within a few nanoseconds and there is no explanation for this loss [4]. The use of the isomeric probe will help to clarify the situation.

2. Experimental

2.1. Sample Preparation

We neutron-activated 100 mg of HfO_2 powder, enriched in ^{179}Hf by 73.7%, in the research reactor BER II at the Hahn-Meitner-Institut, Berlin, Germany, for 20 min. The sample contained 20% ^{180}Hf. We obtained about 17 MBq of ^{180m}Hf and 1 MBq of ^{181}Hf, respectively. The sample was transported to Leipzig where the preparations were carried out. The powder was dissolved in excess 38% HF. With a small part of the liquid we determined the effective anisotropy with our 6-detector camera setup [5], as described below. The liquid was allowed to dry slowly under an IR lamp at about 40 °C. Several small colourless crystals formed and were transferred to a closed polyethylene sample tube in order to avoid a possible slow conversion to $HfF_4 \cdot 3H_2O$ due to humidity in the air. After about 5 h we added another crystal to the sample for the TDPAC measurements in order to increase the coincidence count rate. No further characterization of the sample was carried out because the TDPAC measurement using ^{181}Hf(β^-)^{181}Ta after ^{180m}Hf had decayed allowed an unambiguous determination of the sample composition based on previous studies [4].

2.2. Properties of the Nuclear Probes ^{180m}Hf and ^{181}Hf(β^-)^{181}Ta and Theory

The excited states of the even-even nucleus ^{180}Hf are rotational excitations up to 8^+ followed by an 8^- state at 1.1422 MeV with a half life of 5.5 h. In principle one could use the 4^+ to 2^+ transition with $E_\gamma = 215.3$ keV as start and the 2^+ to 0^+ transition with $E_\gamma = 93.3$ keV as stop. Moreover, in this stretched cascade, other coincidences like the 6^+ to 4^+ transition with $E_\gamma = 332.5$ keV could serve as start with the 4^+ to 2^+ transition being unobserved and yield exactly the same anisotropy, namely $A_{22} = +10.2\%$. This is even true if the 8^- to 6^+ transition with $E_\gamma = 501.2$ keV is used as start, and both the 6^+ to 4^+ transition and the 4^+ to 2^+ transition remain unobserved. Thus it is tempting to allow all lines but the 93.3 keV line as start signals. However, since all transitions preceding the 93.3 keV transition are essentially prompt, a multi-detector spectrometer with hardware coincidences and router gets paralyzed because triple and higher coincidences occur and cannot be routed correctly. The 8^- to 8^+ transition with $E_\gamma = 57.5$ keV as

start signal would yield almost $A_{22} = 17\%$ – assuming a pure E1 transition – but is not useful because of poor time resolution properties and interference with K X-rays at 65.35 keV. For these reasons we have chosen the 501.2 keV (332.5 keV)(215.3 keV) 93.3 keV cascade with the lines in brackets being unobserved. This has the additional advantage that the time resolution is optimized and Compton background interferences are absent. We obtained a time resolution of approximately 800 ps (FWHM), sufficiently good for the present purpose.

The first excited state used for the determination of the NQI has a half life of 1.5 ns and a nuclear quadrupole moment of $Q = -2.00(2)$ b [6]. The powder perturbation function for $I = 2$ reads [3]

$$\begin{aligned} G_{22}(t) = \frac{1}{35}\big[&10 + 2(1-\alpha)\cos\omega_1 t + 3\cos\omega_2 t \\ &+ (2-\alpha(1+\eta))\cos\omega_3 t + (2-\alpha(1-\eta))\cos\omega_4 t \\ &+ (2+\alpha(1-\eta))\cos\omega_5 t + 3\cos\omega_6 t + 3\cos\omega_7 t \\ &+ (2+\alpha(1+\eta))\cos\omega_8 t + 2(1+\alpha)\cos\omega_9 t \\ &+ 4\cos\omega_{10} t\big] \end{aligned}$$

with $\omega_1 = 6(\alpha^{-1} - 1)$, $\omega_2 = 6\eta$, $\omega_3 = 6\alpha^{-1} - 3(1+\eta)$, $\omega_4 = 6\alpha^{-1} - 3(1-\eta)$, $\omega_5 = 6\alpha^{-1} + 3(1-\eta)$, $\omega_6 = 9 - 3\eta$, $\omega_7 = 9 + 3\eta$, $\omega_8 = 6\alpha^{-1} + 3(1+\eta)$, $\omega_9 = 6(\alpha^{-1} + 1)$, $\omega_{10} = 12\alpha^{-1}$ and $\alpha = (1 + \eta^2/3)^{-1/2}$.

Here, as also below, frequencies are in units of

$$\omega_Q = eQV_{zz}/(\hbar 4I(2I-1)). \quad (1)$$

V_{zz} denotes the largest component of the electric field gradient (EFG) tensor in magnitude.

We did not use the $G_{44}(t)$ perturbation function because the anisotropy $A_{44} = +0.0091$ is small compared to A_{22} and is further strongly reduced by solid angle correction factors for our spectrometer arrangement (see below).

The properties of the standard nuclear probe $^{181}Hf(\beta^-)^{181}Ta$ are the following: the cascade 133 keV as start and 482 keV as stop has an anisotropy of $A_{22} = -27.5\%$, the intermediate $I = 5/2$ state has a half life of 10.6 ns and a nuclear quadrupole moment of $Q = +2.35(6)$ b [6], and the perturbation function reads [3]

$$G_{22} = a_0 + a_1\cos\omega_1 t + a_2\cos\omega_2 t + a_3\cos\omega_3 t \quad (2)$$

with $a_0 + a_1 + a_2 + a_3 = 1$ and $\omega_3 = \omega_1 + \omega_2$. All amplitudes and frequencies depend on η. For $\eta = 1$, ω_1 and ω_2 coincide and ω_3 is twice as large.

The analytical formulae are too clumsy to be reproduced here [3]. Again, we restricted the analysis to the $G_{22}(t)$ terms only because A_{44} is small and further reduced by solid angle correction factors. The time resolution for this cascade was approximately 750 ps (FWHM).

It should be noted that the two nuclear probes have the opposite order of start and stop quanta: in ^{180m}Hf we start with the high energy quantum and in $^{181}Hf(\beta^-)^{181}Ta$ with the lowest quantum (except the X-ray line). Thus there is no interference between both cascades due to insufficient separation of the 501.2 keV line and the 482 keV line as well as Compton background from the 133 keV line in the 93.3 keV window. In other words, the delayed coincidences are recorded left and right of the $t = 0$ channel. We could gradually see the build-up of the 10.6 ns decay of ^{181}Hf at negative times compared to the 1.5 ns decay of ^{180m}Hf as their relative activities varied. After the ^{181}Hf had decayed we adjusted the single channel analyzers to the start and stop lines of $^{181}Hf(\beta^-)^{181}Ta$ to continue the measurement with this probe.

2.3. TDPAC Spectrometer

We used the 6-detector TDPAC camera as described elsewhere [5]. The detectors were equipped with conically shaped cylindrical BaF_2 scintillators of 44 mm diameter and 44 mm height. The cone angle was $2 \times 54.7^\circ$ such that the six detectors, arranged along Cartesian coordinates, could touch each other thus minimizing the source detector distance. As shown before, under these conditions the information gain is optimized [5]. The large acceptance angle guarantees the registration of as many coincidences as possible (we roughly cover 10% of 4π solid angle per detector); at the same time the solid angle correction factors reduce the theoretical anisotropy by about 50%. In the present geometry we slightly increased the source detector distance for technical reasons and the reduction factors of the anisotropy were determined by liquid samples.

3. Results

3.1. ^{180m}Hf as Probe

We performed two independent measurements at 300 K for both cascades and obtained reproducible results. In order to improve the statistical accuracy, the data for the ^{180m}Hf measurement were added for the

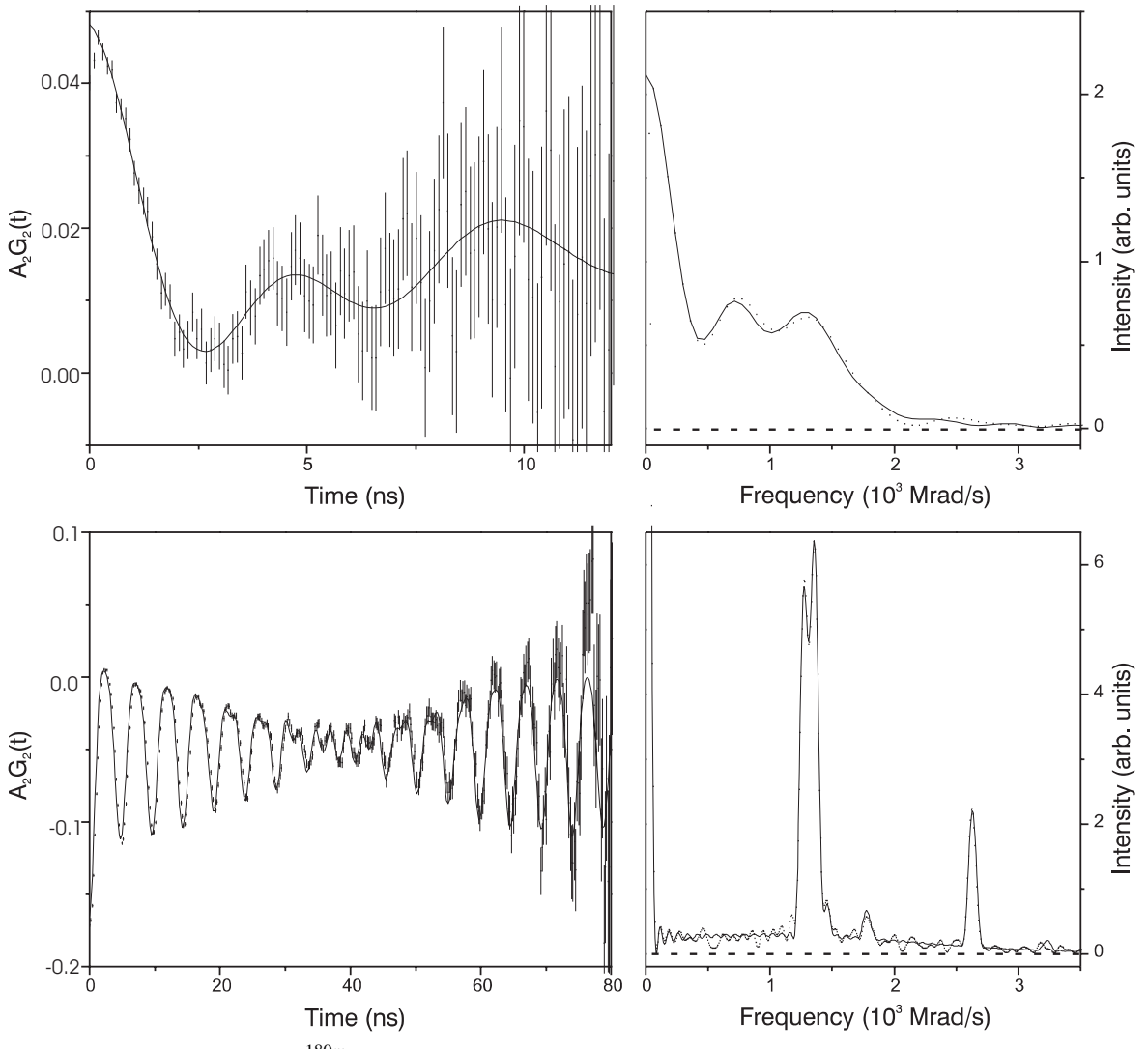

Fig. 1. Top: TDPAC spectrum of ^{180m}Hf in $HfF_4 \cdot HF \cdot 2H_2O$ (left) and its cosine transform (right). Bottom: TDPAC spectrum of ^{181}Hf(β^-)^{181}Ta in $HfF_4 \cdot HF \cdot 2H_2O$ (left) and its cosine transform (right). Note the very broad peak under the sharp ones. Texture in the sample is revealed by the intensities of the double peak. There is a small foreign phase revealed by peaks around 1.45 and $1.8 \cdot 10^3$ Mrad/s which is tentatively attributed to $Hf_2OF_6 \cdot H_2O$.

least squares fit analysis. This was not necessary for the ^{181}Hf(β^-)^{181}Ta measurements. We started with the determination of the effective anisotropy, i. e. the solid angle correction factors, for ^{180m}Hf using a liquid sample. We obtained $A_{22} = +4.5(2)\%$ which means that the solid angle correction factor is $Q_{22} = 0.44(2)$. This was reproduced by a second measurement of a new sample. After that we took a few crystals and started the measurement on $HfF_4 \cdot HF \cdot 2H_2O$. After about 5 h we added about the same amount of activity in order to improve the statistics. After 24 h we stopped data taking with this probe. The time spectrum of ^{180m}Hf as probe (both experiments added) is shown in Fig. 1 (top, left) together with its cosine transform (top, right). The spectrum reveals two frequencies – in fact two unresolved groups of frequencies – apart from the time-independent hardcore. Due to pile-up problems there was a small baseline shift which we subtracted from the data. The first two channels are corrupted by minute inaccuracies of the time-zero determination and were excluded in the least squares fit analysis. The spectrum is unambiguously fitted using (1) including

Table 1. Hyperfine parameters for ^{180m}Hf in $HfF_4 \cdot HF \cdot 2H_2O$.

Parameter	Assumed distribution	
	Lorentzian	Gaussian
A_{22}^{eff} (%)	+4.96(11)	+4.97(31)
ω_Q (Mrad/s)	103(4)	105(6)
η	0.68(3)	0.66(3)
δ (%)	7.3(3.9)	16(7)
χ^2	0.553	0.534

finite time resolution corrections with the parameters listed in Table 1.

Least squares fits were performed assuming a Lorentzian and a Gaussian frequency distribution. The χ^2 value does not help to differentiate between both distribution functions. The χ^2 values are small because we fitted the entire range until 12 ns. In any case, the two types of analysis give confidence in the fitted parameters, the apparent discrepancy in the line-broadening parameters is merely a result of the fact that δ enters quadratically in the case of a Gaussian distribution whereas it enters linearly for a Lorentzian distribution. Both values indicate little line broadening.

3.2. *^{181}Hf(β^-)^{181}Ta as Probe*

After completion of the experiments with ^{180m}Hf we continued the measurements with ^{181}Hf(β^-)^{181}Ta as probe. First, we measured the effective anisotropy using a liquid sample. We obtained $A_{22}^{\text{eff}} = -16.1(6)\%$ and thus got $Q_{22} = 0.59(2)$. The activity was sufficiently strong to get enough statistics within a few hours. We then changed to the $HfF_4 \cdot HF \cdot 2H_2O$ sample and collected data for several days. The time spectrum is shown in Fig. 1 (bottom, left) together with its cosine transform (bottom, right). Again, we subtracted a small base-line shift. It is immediately obvious that a sort of beat pattern prevails which indicated an asymmetry parameter close to unity. It is also obvious that the initial anisotropy starts at about -17%, as expected, but is lost partly within the first few nanoseconds. In other words, there is a rather broad frequency distribution under the sharp double-peak with a significant area. A least squares fit analysis gave the results listed in Table 2 which are compared to those previously reported in [4].

The values for χ^2 are very similar and do not allow to discriminate between the two distribution functions. All fitted hyperfine parameters are practically the same for Lorentzian and Gaussian broadening with the exception of the distribution parameter δ, the origin of which was already discussed above. We allowed for a small shift of t_0 which we attribute to small drifts during the long data collection time. In addition, we noticed that the line intensities differed slightly from the values for random powder samples. This is attributed to the fact that we used only a few crystallites which could have led to preferred orientation (texture). Therefore we allowed the amplitudes to adjust freely for fraction 1. For the other fractions this extra freedom was irrelevant. This had no effect on fitted frequencies and asymmetry parameters but merely improved the χ^2 value. This effect would in principle also show up in the ^{180m}Hf spectra but is much too small to be visible there.

Table 2. Hyperfine parameters for ^{181}Hf in $HfF_4 \cdot HF \cdot 2H_2O$.

Parameter	This work	[4]
Assumed Lorentzian distribution:		
χ^2	0.98	?
A_{22}^{eff} (%)	−18.2(3)	−23.0(1)
Fraction 1 (%)	53.2(8)	62(1) (A), 55(1) (B)[a]
ω_Q (Mrad/s)	126.69(4)	126.86(31)
η	0.9243(4)	0.927(1)
δ (%)	0.11(3)[b]	0.6(1)
Fraction 2 (%)	4.6(4)	15(1)
ω_Q (Mrad/s)	161.8(3)	159.4(2.2)
η	0.762(4)	0.71(2)
δ (%)	0[c]	9(2)
Fraction 3 (%)	39.0(7)[d]	not modelled
ω_Q (Mrad/s)	109.3(3.7)	
η	1[e]	
δ (%)	81(3)[b]	
Assumed Gaussian distribution:		
χ^2	0.953	not analyzed
A_{22}^{eff} (%)	−19.0(5)	
Fraction 1 (%)	56.5(7)	
ω_Q (Mrad/s)	126.64(4)	
η	0.9241(4)	
δ (%)	0.40(8)[f]	
Fraction 2 (%)	4.6(4)	
ω_Q (Mrad/s)	161.7(3)	
η	0.761(4)	
δ (%)	0[c]	
Fraction 3 (%)	39.0(7)[d]	
ω_Q (Mrad/s)	112.2(2.9)	
η	1[e]	
δ (%)	81(3)[f]	

[a] Two samples. [b] Assumed Lorentzian. [c] Assumed. [d] Accounts for a rapid loss of anisotropy modelled by the associated parameters. [e] Fixed. [f] Assumed Gaussian.

4. Discussion

To our knowledge, this is the first experiment using the isomeric nuclear probe ^{180m}Hf for a TDPAC study. Apart from the proof of feasibility, the comparison with the more common probe ^{181}Hf(β^-)^{181}Ta al-

lows to answer the question why part of the anisotropy is lost within a few nanoseconds for the latter probe in $HfF_4 \cdot HF \cdot 2H_2O$.

First, the results with the nuclear probe ^{180m}Hf will be discussed. The observed effective anisotropies A_{22} are slightly larger than the one obtained with the liquid sample. Also, there is a small but non-negligible frequency distribution which should be absent if all nuclear probes experience exactly the same EFG. Both observations are likely related. We noticed that the fitted linewidth increased with increasing data collection time. Since we have no indication that the sample changed during 24 h [and even several days, as revealed by the subsequent measurement using ^{181}Hf(β^-)^{181}Ta] we attribute this to a gradual build-up of a prompt contribution from the 482 keV line in the 501.2 keV window and the K X-ray at 65.35 keV in the 93.3 keV window. With this in mind, the effective anisotropy A_{22}^{eff} is probably slightly overestimated and, hence, the fit requires a small damping. Within the experimental accuracy of about 5% we observe the full anisotropy for the present geometry. With the nuclear quadrupole moment for the 2^+ state of $Q = -2.00(2)$ b and taking the average for ω_Q from both lineshape analyses we derive $V_{zz} = \pm 8.2(5) \cdot 10^{22}$ V/m^2, where the uncertainty in ω_Q contributes the majority to the error limits.

Turning now to the results with the nuclear probe ^{181}Hf(β^-)^{181}Ta it is clear that the beat pattern corresponds to a well-defined phase which we identify with $HfF_4 \cdot HF \cdot 2H_2O$ based on previous studies [4]. Although Rickard and Waters [7] stated that the HF adduct does not exist for hydrated HfF_4, it is described by Gaudreau [7] and we have monitored the slow conversion from $HfF_4 \cdot HF \cdot 2H_2O$ to $HfF_4 \cdot 3H_2O$ [8]. It thus might have escaped the observation of Rickard and Waters in case they stored their samples in humid air for longer periods. It constitutes, however, only a bit more than 50% of all probe nuclei. The small admixture of roughly 5% is tentatively identified as $Hf_2OF_6 \cdot H_2O$ according to previous studies [4]. It is barely visible as a small shoulder on the high frequency side of the double peak and a small corresponding harmonic around 1800 Mrad/s. It is not clear whether this phase is formed right away from the beginning or whether it gradually develops with time. In any case, it would have been too small to be detectable in the ^{180m}Hf spectrum. The quoted fractions have to be taken with some precautions because the effective anisotropy A_{22}^{eff} obtained from the least squares fit is slightly larger [$-18.2(3)$% for Lorentzian distribution to $-19.0(5)$% for Gaussian distribution] than the value obtained from the liquid sample [$-16.1(6)$%]. This probably reflects to some extent that neither the Gaussian nor the Lorentzian frequency distribution are completely adequate. In any case, it is clear that the discrete component in the spectrum contributes only with about half of the total anisotropy. It should be mentioned that the present results are in excellent agreement with those previously reported [4], both as far as the observed frequencies and asymmetry parameters are concerned as well as the observed fraction for the principal component (see Table 2). The larger A_{22}^{eff} in [4] is certainly due to the larger source-detector distance when the standard cylindrical scintillators are used whereas we used conically capped cylinders which allow a shorter source-detector distance. The present sample revealed a smaller broadening of the main component and a smaller fraction 2 for the foreign phase. The main difference between the earlier work [4] and the present work is that the "missing fraction" was not analyzed in the earlier work; the fit simply started later and the accuracy was probably insufficient for further analysis. As will be discussed below, we shall analyze this missing fraction in more detail.

With the nuclear quadrupole moment for the 5/2 state of $Q = 2.35(6)$ b and taking the average for ω_Q from both lineshape analyses we derive $V_{zz} = \pm 1.42(4) \cdot 10^{23}$ V/m^2 where the uncertainty is practically given by the uncertainty of Q. When comparing this result with that of the ^{180m}Hf probe we note that the EFG at the Ta nucleus is about a factor of 1.73 larger than that at the Hf nucleus which is certainly not explainable by different quadrupolar polarizibilities of the ion cores (Sternheimer factors γ_∞). It means that the electron density around the probe nucleus is rather different. Moreover, it could happen that the coordination geometry has changed after nuclear transmutation. The rather large EFG suggests that the coordination polyhedron is far from being regular. When comparing the values for the asymmetry parameter, i. e. $\eta = 0.66$ and 0.9243 for ^{180m}Hf and ^{181}Hf(β^-)^{181}Ta probes, respectively, it is also unlikely that the bonds to fluoride ions remain unchanged. This, however, can also be true for the HF adduct and perhaps also for the two water molecules, none of them forming a bond with the metal. In this context it is interesting to note that tetrafluorides of Ta are not known, but those of Nb [9]. In other words, after transmutation the Ta atom is in unfavoured coordination.

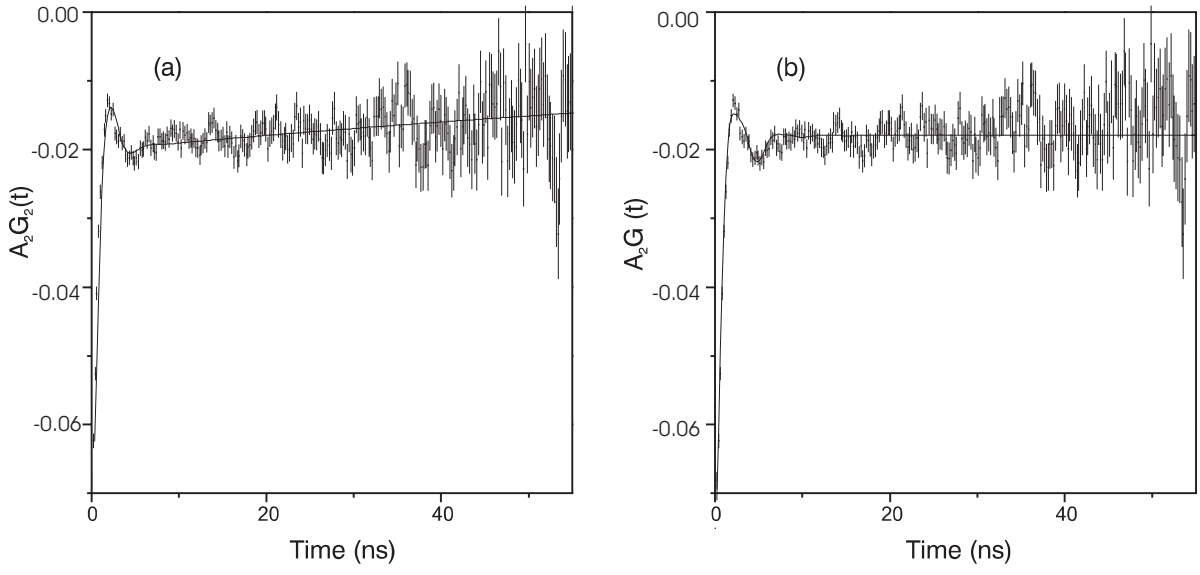

Fig. 2. Residual TDPAC spectrum of $^{181}Hf(\beta^-)^{181}Ta$ in $HfF_4 \cdot HF \cdot 2H_2O$ after subtraction of the discrete fractions 1 and 2 in an expanded view. (a) Fit with a perturbation function consisting of a static perturbation function with a broad frequency distribution, multiplied by a common exponential factor $\exp(-\lambda t)$. (b) Fit with a perturbation function consisting of a static perturbation function without frequency distribution, multiplied by a common exponential factor $\exp(-\lambda t)$.

This idea could possibly help in explaining why roughly 40% of all probe nuclei experience an interaction which was modelled by an extremely broad distribution. The origin of the distribution could be a static inhomogeneity or it could be due to a fluctuating interaction. In order to discriminate between both possibilities we subtracted both discrete components (fraction 1 and 2) and analyzed the residual in more detail. Figure 2 shows that the residual consists of a rapid decrease of anisotropy, followed by a small recovery. We fitted this residual with two types of perturbation functions.

First, a perturbation function consisting of a static perturbation function with a broad frequency distribution which is multiplied by a common exponential factor $\exp(-\lambda t)$ was used. In this case, we obtained $\delta = 0.74(2)$ for a Gaussian distribution and $\delta = 0.63(2)$ for a Lorentzian distribution and $\lambda = 0.0047(6)\ \mathrm{ns}^{-1}$ and $\lambda = 0.0071(6)\ \mathrm{ns}^{-1}$, respectively (see Fig. 2a). The fitted frequency was $\omega_Q = 116(3)$ Mrad/s, not too far from that of the principal component. The asymmetry parameter was kept fixed at $\eta = 1$. In other words, most of the broadening is due to static inhomogeneities and relaxation effects are rather slow.

An alternative way to fit this residual is with a perturbation function consisting of a static perturbation function without a frequency distribution which is multiplied by a common exponential factor $\exp(-\lambda t)$. We obtained $\lambda = 0.55(2)\ \mathrm{ns}^{-1}$ (see Fig. 2b), a relaxation rate two orders of magnitude larger compared to the first approach. The fitted frequency was $\omega_Q = 131(6)$ Mrad/s, again not too far from that of the principal component. Hence, we require that the relaxation is still in the slow relaxation regime, i. e., $\omega_Q \tau_c < 1$ with τ_c denoting the correlation time, but close to the cross-over to the fast relaxation regime. This means that τ_c should be of the order of 10 ns.

In principle it would be possible to discriminate between both cases by the inspection of the long-time behaviour: for the first case, the anisotropy decreases very slowly whereas in the latter case it goes to zero rapidly. Unfortunately, due to the texture of the sample, we had to allow for a freely adjustable "hardcore", i. e., the time-independent part of the perturbation function, and thus have no further criterion for the discrimination. The values for χ^2 were also very similar for both cases.

The second scenario requires one parameter only whereas the first needs two and the origin of the broad static distribution remains unclear. Both perturbation functions are likely to be crude approximations to the result for the correct relaxation Hamiltonian only. We favour the second scenario because of the simplicity but cannot exclude the first one.

Since the start level of the cascade in ^{181}Ta is long-lived (17.8 μs) we require a steady state situation rather than an irreversible process which immediately follows the transmutation.

It seems possible that we are dealing with a fluctuating EFG due to mobile HF molecules or H_2O molecules. If the EFG fluctuates in magnitude and orientation with a rate of order 10^8 s^{-1} it could lead to a rapid loss of anisotropy. The reason why we observe two fractions could possibly be dictated by the additional water molecules. In fact, there are wide stoichiometry ranges for the water content in Hf-tetrafluoride [7], and we have noticed that the exact value of the discrete fraction depends slightly on sample preparation, as observed before [4].

A natural consequence to test this hypothesis is to carry out temperature-dependent studies. This has been done in the temperature range from 77 K up to the dehydration/decomposition temperature around 373 K without getting a clear answer. There were small variations in the fractions and in the line broadening which did not allow to extract activation energies for the proposed processes. We only observed some line broadening at 77 K. Thus we do not consider this a likely process, especially in view of the fact that neither the water nor the HF molecules bind to the metal.

It helps to discuss the fate of the Ta atom after nuclear transmutation. We certainly had tetravalent Hf(IV) and a high degree of ionicity, i. e., the Hf atom has a closed shell configuration. After transmutation Ta could either remain in a pentavalent state or capture an electron to convert to Ta(IV). If the latter is the case, a redox reaction together with hydrolysis could take place of the type $Ta(IV)F_4+H_2O \rightarrow Ta(V)OF_3+HF+H$. If the Ta atoms capture one electron and subsequently convert to Ta(V) by the abovementioned reaction, the discrete fraction in the spectrum would correspond to the reaction product whereas the residual would correspond to the host without redox reaction/hydrolysis. Ta(V) occurs in about 55% of all cases whereas in the remaining 40% the Ta atoms remain in their tetravalent state with $5d^1$ configuration carrying a magnetic moment. This leads to a rapidly fluctuating magnetic dipole interaction combined with a rapidly fluctuating electric quadrupole interaction. The magnitude of the fluctuating magnetic field can be estimated as follows. The magnetic field produced by a 5d electron is -55 T [10] and the magnetic moment of the $I = 5/2$ state is 3.29 μ_N [6], which leads to a magnetic splitting of about 5.7 μeV. The magnitude of the fluctuating electric field gradient can be estimated as follows. For a 5d electron we have $\langle r^{-3} \rangle$ of the order of $4 \cdot 10^{31}$ m^{-3} [11], which yields for a $5d_{z^2}$ electron an EFG of the order of $3 \cdot 10^{22}$ V/m^2. With the nuclear quadrupole moment of the $I = 5/2$ state $Q = 2.36$ b we obtain $eQV_{zz}/(4I(2I-1))$ of about 0.2 μeV. In the fast relaxation limit we have an exponential loss of anisotropy with a relaxation rate $\gamma_2 = 2\omega_L^2\tau_c$ for the magnetic case and a $\gamma_2 = 100.8\omega_Q^2\tau_c$ for the quadrupole case [12]. Here, ω_L is the Larmor frequency. In the limit of $\omega\tau_c = 1$ we finally obtain $\hbar\omega_L = 11.4$ μeV and $\hbar\omega_Q$ about 20 μeV. This means that both interactions are of comparable strength. In fact the estimates given above are about an order of magnitude larger than required experimentally. This is not surprising regarding the crude approximations made.

The question remains why about 40% of the probe nuclei are subjected to this fluctuating magnetic field/electric field gradient and about 55% are not. Whereas the formation of $Ta(V)OF_3$ is probably energetically favoured, its stability could be modified if embedded as isolated defect in the $HfF_4 \cdot HF \cdot 2H_2O$ matrix. It is interesting to note that for $HfF_4 \cdot 3H_2O$ we observe about $2/3$ of a discrete signal and about $1/3$ of the anisotropy is lost rapidly [8]. A previous study [13] of this compound did not quote A_{22}^{eff}, but the spectra looked like ours and started with about -15% anisotropy which, compared to assumed $A_{22}^{\text{eff}} = -23.0(1)\%$ as in [4], would also give about $2/3$ of the total anisotropy for the discrete component.

It should also be mentioned that there are many unexplained observations with the probe $^{181}Hf(\beta^-)^{181}Ta$ in Hf/Zr compounds which may have similar origins. (i) HfS_2 revealed nuclear quadrupole frequency doubling [14] which still lacks an explanation; (ii) $HfSe_2$ exhibited a splitting and strong line broadening when cooling to 10 K [15]; (iii) ZrS_2 exhibited a very strong temperature dependence of the EFG of the order of 1 Mrad/s per 1 K and, upon cooling down from 1200 K, separated into two branches, one being close to the original one and the other approaching more that of HfS_2 [14], thus suggesting disproportionation. In all cases the axial symmetry at the probe is broken in certain temperature ranges although the host lattices have a tree-fold rotation axis at the metal sites. These features have previously been associated with lattice instabilities around the probe atom. Based on the experience with the present study we now believe that they are associated with the chemistry of the Ta impurity in these group IVb compounds which possibly

includes features like disproportionation, metal-metal bond formation, or paramagnetic centre formation, and thus apparently is much richer than anticipated. The situation with $HfTe_5$ might be different because the resistance anomaly as a function of temperature which is accompanied by an anomaly of the hyperfine parameters can be suppressed by lattice defects [16]. Here, we are dealing with bulk electronic effects, most likely in the Te zigzag chain, and the impurity probe is not responsible for the resistance anomaly.

Summing up, the comparative study of $HfF_4 \cdot HF \cdot 2H_2O$ with ^{180m}Hf and $^{181}\mathrm{Hf}(\beta^-)^{181}$Ta as probes revealed that $^{181}\mathrm{Hf}(\beta^-)^{181}$Ta is not an "innocent spy" as is commonly assumed. It would pay off to investigate more Hf compounds with both nuclear probes sequentially, especially those where the observed effective anisotropy is too low. However, such investigations would be restricted to cases where the EFGs are large. A cross-check would be an experiment with the hcp metal Hf. It would have to be ultrapure Hf (say < 100 ppm Zr) because there is ample evidence that the Ta-Zr impurity pair leads to a broken symmetry at the Ta site [17].

5. Outlook

As mentioned above, a multi-detector setup with hardware coincidence and routing is paralyzed when all quanta feeding the 2^+ state were used as starts. This difficulty can be overcome when the detector signals are digitized with time stamps and the coincidence and routing is performed by software. Such a fully digital TDPAC spectrometer is under construction and will be extremely useful for further experiments with the new "spy" ^{180m}Hf. Moreover, experiments with natural isotopic abundance seem feasible.

In the search for a plutonium analogue, $^{181}\mathrm{Hf}(\beta^-)^{181}$Ta in chelate complexes was used for binding studies to transferrin [18]. In order to mimic the interaction of Pu with biomolecules, metallic or oxidic analogues would be much more relevant than chelates. Here, ^{180m}Hf could turn out to be useful.

Acknowledgement

The neutron activations were kindly carried out at the Forschungsreaktor BER II at the Hahn-Meitner-Institut, Berlin, Germany. We thank Dr. Thomas Agne for his help with sample activation and transport. It is a pleasure to thank Prof. Dr. Harald Krautscheid and Prof. Dr. Fred Jochen Litterst for fruitful discussions and Mr. Steffen Jankuhn for his help with the preparation of the manuscript.

[1] A. Lerf and T. Butz, Hyperfine Interact. **36**, 275 (1987).
[2] R. B. Firestone and V. S. Shirley (Eds.), Table of Isotopes, 8th ed., John Wiley and Sons, New York 1996.
[3] T. Butz, Hyperfine Interact. **73**, 387 (1992).
[4] W.-G. Thies, H. Appel, R. Heidinger, and G. Then, Hyperfine Interact. **30**, 153 (1986) (and references therein).
[5] T. Butz, S. Saibene, T. Fraenzke, and M. Weber, Nucl. Instrum. Methods A **284**, 417 (1989).
[6] N. J. Stone, At. Data Nucl. Data Tables **90**, 75 (2005).
[7] C. E. F. Rickard and T. N. Waters, J. Inorg. Nucl. Chem. **26**, 925 (1964) (for $HfF_4 \cdot 3H_2O$); M. B. Gaudreau, C. R. Acad. Sci. Ser. C **263**, 67 (1966) (for $HfF_4 \cdot HF \cdot 2H_2O$).
[8] S. K. Das, C. C. Dey, S. Dey, and T. Butz, to be published.
[9] A. F. Hollemann and F. Wiberg, Lehrbuch der organischen Chemie, Walter de Gruyter, Berlin 2007.
[10] C. E. Johnson, in: Hyperfine Interactions in Excited Nuclei (Eds. G. Goldring and R. Kalish), Gordon & Breach Sci. Publ., New York 1971, Vol. 3, p. 803.
[11] J. P. Desclaux, At. Data Nucl. Data Tables **12**, 311 (1973).
[12] H. Winkler and E. Gerdau, Z. Phys. **262**, 363 (1973).
[13] J. A. Martínez, M. C. Caracoche, A. M. Rodríguez, P. C. Rivas, and A. R. López García, Chem. Phys. Lett. **102**, 277 (1983).
[14] T. Butz, A. Hübler, and A. Lerf, Phys. Rev. B **26**, 3973 (1982).
[15] T. Butz, A. Lerf, A. Hübler, S. Saibene, and G. M. Kalvius, Hyperfine Interact. **20**, 268 (1984).
[16] S. Saibene, T. Butz, A. Lerf, and W. Biberacher, Hyperfine Interact. **35**, 255 (1987).
[17] R. L. Rasera, R. C. Reno, G. Schmidt, T. Butz, A. Vasquez, H. Ernst, G. K. Shenoy, and B. D. Dunlap, J. Phys. F Met. Phys. **8**, 1579 (1978).
[18] G. Then, H. Appel, J. Duffield, D. M. Taylor, and W.-G. Thies, J. Inorg. Biochem. **27**, 255 (1986).